IMAGE & SIGNAL PROCESSING

Upper Limb Movement Classification Via Electromyographic Signals and an Enhanced Probabilistic Network

Alexis Burns[1] · Hojjat Adeli[2] · John A. Buford[3]

Abstract

Few studies in the literature have researched the use of surface electromyography (sEMG) for motor assessment post-stroke due to the complexity of this type of signal. However, recent advances in signal processing and machine learning have provided fresh opportunities for analyzing complex, non-linear, non-stationary signals, such as sEMG. This paper presents a method for identification of the upper limb movements from sEMG signals using a combination of digital signal processing, that is discrete wavelet transform, and the enhanced probabilistic neural network (EPNN). To explore the potential of sEMG signals for monitoring motor rehabilitation progress, this study used sEMG signals from a subset of movements of the Arm Motor Ability Test (AMAT) as inputs into a movement classification algorithm. The importance of a particular frequency domain feature, that is the ratio of the mean absolute values between sub-bands, was discovered in this work. An average classification accuracy of 75.5% was achieved using the proposed approach with a maximum accuracy of 100%. The performance of the proposed method was compared with results obtained using three other classification algorithms: support vector machine (SVM), k-Nearest Neighbors (k-NN), and probabilistic neural network (PNN) in terms of sEMG movement classification. The study demonstrated the capability of using upper limb sEMG signals to identify and distinguish between functional movements used in standard upper limb motor assessments for stroke patients. The classification algorithm used in the proposed method, EPNN, outperformed SVM, k-NN, and PNN.

Keywords Upper Limb Movement Classification · EMG · Electromyographic Signals · Enhanced Probablistic Neural Network · Surface EMG · Semg · Machine learning · Wavelet transform · Motor rehabilitation

Introduction

Surface electromyographic (sEMG) signals are electrical potentials in the muscles during movement that are acquired by

✉ Hojjat Adeli
adeli.1@osu.edu

Alexis Burns
alexis.meashal@gmail.com

1 Department of Biomedical Engineering, The Ohio State University, Columbus, OH 43210, USA

2 Departments of Biomedical Engineering, Biomedical Informatics, Neurology, and Neuroscience, The Ohio State University, Columbus, OH 43210, USA

3 Physical Therapy Division, School of Health and Rehabilitation Sciences, The Ohio State University, 453 W 10th Ave, Rm. 516E, Columbus, OH 43210, USA

electrodes applied on the surface of the skin [8, 16]. These signals are generated by the brain and transmitted and optimized through neural pathways and networks to produce the appropriate muscle activation patterns for both voluntary and involuntary movement. There are invasive and non-invasive methods of acquiring EMG signals. Needle and fine wire electrodes have been used to acquire intramuscular EMG signals by penetrating the layers of the skin and being in direct contact with the muscle fibers. Due to their invasive nature, intramuscular EMG recordings are limited to being applied in clinical settings and only when absolutely necessary. sEMG is non-invasive and uses Ag/AgCl disposable electrodes on the surface of the skin. While this method has a lower signal acquisition resolution due to the distance of the electrode from the actual muscle, it is preferred in most applications and by most patients.

The advancement of machine learning techniques has propelled the field of technology in the last decade [13, 18, 32, 47, 52, 64]. Recent algorithms such as random forest classification [6, 61], particle swarm optimization [2, 55], deep learning [23, 60], and convolutional neural networks [4, 33, 35, 37, 50, 51, 57–59] have outperformed earlier methods such as the

support vector machine [5, 65], principal component analysis [7, 15, 42], and linear discriminant analysis [40, 56] in many applications. When applied to muscle signals, the aforementioned techniques have been utilized to classify movements and to detect muscle activation abnormalities ([11, 17, 29]).

The purposes of sEMG are many. In biomechanics studies, the goals are typically to determine which muscles are active during a particular task, when they are active and when they are not, and how strongly they are activated. Another application of sEMG is to attempt to discern what movement is being performed, and potentially, how well the movement is being performed. Motion capture and analysis is currently the only reliable way to measure movement [27]. It requires complex systems, such as multi-camera motion tracking, acceleration and orientation electrodes, and a variety of other approaches that typically demand a full-blown biomechanics research laboratory. These approaches are complex, expensive, time-consuming and labor intensive, and not suitable for most clinical applications. Surface EMG, in comparison, is relatively simple to apply. A wearable technology with an embedded machine learning algorithm can analyze sEMG signals from the upper limb to determine what movements are being performed and to grade the quality of movement in real time. Such a device can provide objective and consistent analysis of progressive motor improvements, providing clinicians with objective, real time information about the effectiveness of various treatment approaches. This could prove useful not only in research settings to test new therapies, but also in clinical use to guide clinical decision making. Martinez-Mozos et al. [34] use wearable physiological sensors for stress detection.

Automated analysis of movement is of high importance for neurological disorders and injuries that cause motor impairment. Much of the literature regarding machine learning for sEMG has been dedicated to enhancing myoelectric control of robotic arms, specifically for amputee patients [5, 6]. Other neurological disorders that have been targeted in the literature for sEMG machine learning include amyotrophic lateral sclerosis (ALS) [44] and stroke [36]. However, these have been explored less in the literature compared to the targeted amputee population. Each of these populations has different needs when it comes to movement classification. Many ALS patients are unable to make any movement at all, and therefore, classifying movement is not a priority. Within the literature regarding this target population, sEMG is used to identify specific signatures within the signal that can be used for diagnosis of ALS [44]. On the other hand, many amputees maintain control of their upper arm and some of their forearm, which enables them to complete larger movements, known as gross motor functions, with the shoulder and elbow joint. Because the hand has been amputated, fine motor functions, such as wrist movements, finger movements, and grasps are of the utmost importance to this population. Myoelectric prosthetic arms are robotic arms controlled by sEMG signals to

complete actions amputee patients cannot. Much of the literature focuses on restoring fine motor function to amputee patients using the sEMG signals from the forearm. This differs entirely from the stroke population, which is the target of the present study.

Due to lesions in the brain caused by stroke, stroke patients often lose motor control of one side of their body. Seventy-five percent of stroke survivors lose motor control of their upper limb that persists into the chronic stage [20]. To regain motor function, many stroke patients go through rehabilitative physical and occupational therapy, where therapists use their expert knowledge to rate patient motor dysfunction and response to treatment on a scale based on qualitative criteria. Of the many motor function assessments, among the most popular include the Fugl-Meyer Assessment, Arm Motor Ability Test (AMAT), Wolf Motor Function Test, and Brunnstrom Scale. Based on their level of motor impairment, stroke patients rehabilitate motor function by attempting to perform both gross and fine motor functional movements within a structured rehabilitation program that sometimes uses robotic mechanical assistance to enhance patient movement [30, 46]. An automated and quantitative assessment of motor function identification and quality has been studied in the literature, due to a desire to monitor patients outside of the clinic as well as to quantitatively show motor rehabilitation progression [19, 26, 41].

One way to approach this problem of measuring recovery is to determine ways to automatically classify movement from biosignals. There are multiple techniques within machine learning used in the literature for movement classification via sEMG features. Among the most popular reported are support vector machine (SVM) [5, 6], principal component analysis [7], multilayer perceptron and fuzzy neural networks [45], and linear discriminant analysis [40]. The accuracy of many of these techniques depends heavily on the features chosen to represent the signal characteristics. Because of this, combinations of techniques are used to achieve higher accuracies, for example, with one as an optimizer and the second as the classifier [9]. Used alone, SVM classification is shown to yield poor accuracies for sEMG signals for movement classification, for example, Atzori et al. [5] reports an accuracy of 70% when classifying dynamic upper limb movements for 40 subjects.

Several studies have adjusted the feature set parameters using optimization techniques in order to enhance the accuracy outcomes of SVM. By combining recursive feature elimination to use only the most pertinent features for SVM classification, a recent study reported increasing the accuracy by 3% [48]. A similar study increased their SVM classification accuracy from 8% to 76% by applying non-negative matrix factorization as a pre-processor to SVM [53]. While combining pre-processing methods with SVM does increase the accuracy, it also increases the required processing time, because

these studies used 10 subjects from the same database as Atzori et al. [5] that has 40 subjects total, it has yet to be shown if these combinatory methods will increase the accuracy with more subjects in the pool.

Kinematic and sEMG electrodes have been applied in an attempt to identify characteristics of movement in patients recovering from stroke outside of the clinic, to provide information to mechanical movement assistance robots, and to provide more information to clinicians for diagnosis and treatment. Randomized control trials utilizing wearable technology have changed from solely using accelerometer data [21, 39, 54] to using inertial measurement units (IMUs) for daily movement monitoring in stroke patients ([28]; [36]; Z. [62]). Unfortunately, wearable IMUs are limited to collecting gross motor movements and can be bulky and uncomfortable. sEMG, on the other hand, is capable of collecting data to classify both gross and fine motor movements [5, 45] and is not limited to providing information for movement prediction alone. sEMG can also be analyzed to decipher limb and joint position in space. A recent study reported estimated joint position over time using sEMG [30]. Information provided by sEMG can also be used as a measurement of movement quality. Changes in the sEMG activity in the upper limb have been correlated to motor function improvement based on Fugl-Meyer scores [41].

Only a few studies in the literature report application of the sEMG to movement classification for stroke patients. Lorussi et al. [31] combined an IMU with an sEMG electrode to model shoulder movement with the goal of understanding scapular function during stroke rehabilitation. Liu et al. [30] used sEMG and a non-linear autoregressive exogenous model to classify continuous arm position of elbow, shoulder, and wrist joints with 10 stroke subjects at 98% accuracy. That study, however, used a robotic exoskeleton while collecting sEMG signals, which would help stabilize movements in light of spasticity. Another study attempted to classify free reaching movements in stroke subjects, and reported that an SVM model yielded an average accuracy of 34% [7].

Frequency domain feature extraction using information from the discrete wavelet transform provides a proper depiction of sEMG's non-stationary nature. The enhanced probabilistic neural network (EPNN) has shown promising results in previous studies using biosignals such as electrocardiograms (ECGs) and electroencephalograms (EEGs) [1]. To answer the question, "Can movements used in stroke motor ability assessments be distinguished using EPNN?", this paper presents a method for identification of the upper limb movements from sEMG signals using a combination of digital signal processing, wavelet transform and the enhanced probabilistic neural network. The performance of the proposed method is compared with results obtained using three other classification algorithm: SVM [25], k-Nearest Neighbors (k-NN), probabilistic neural network (PNN) [43].

Methods

NINAPro EMG Data

To test the approach, the authors used a publicly available NINAPro (Non Invasive Adaptive Prosthetics) data source based on movements performed by healthy individuals collected by Atzori et al. [5] (http://ninapro.hevs.ch/). There is no comparable public database of EMG for patients recovering from stroke. Upper limb sEMG data from the open-source NINAPro database 2 during Exercise C were used to validate the model developed in this study. Atzori et al. [5] collected sEMG signals via wireless Ag/AgCl electrode data using 40 different upper extremity movements from 40 healthy, 23–45 years old subjects. Exercise C consisted of 23 different hand grasping movements. Electrodes were placed over the following muscles in the arm: biceps brachii, triceps brachii, extensor digitorum superficialis, and 8 equidistant electrodes around the forearm to capture aggregate muscular signals from small forearm muscles (Fig. 1). The 12 electrodes were spread across the arm above and below the elbow to capture muscle activity while each subject completed 40 different movements, with the expectation that the variance of the sEMG signals for each channel could be used to distinguish between these movements. Sampled at 2 kHz, the NINAPro data includes timestamps for periods of rest and the beginning of each movement. A number associated with the type of movement is also included. These timestamps were crosschecked after recording by Atzori et al. [5].

Illustrated are the positions of wireless Ag/AgCl electrodes on the subjects from the NINAPro Database. Each oval represents an electrode. The sample signals shown are a representation of the raw sEMG signal from each electrode during one movement. Each signal is on a y-axis of 0.001 mV and an x-xis of 6 s.

The AMAT is a widely accepted method for qualitatively assessing a patient's motor ability post-stroke. It consists of 10 movements, which are then broken down into sub-movements for assessment (see Appendix Table 4). To the best of the authors' knowledge there is no database containing upper limb sEMG data during dynamic functional movements from stroke patients. Therefore, five movements were selected from the NINAPro Database 2 that mimicked movements used within the AMAT. Table 1 identifies which five NINAPro movements were selected that corresponded with AMAT gestures. Signal processing, feature extraction and EPNN classification were applied to these five movements for a clinically-relevant application of movement classification for use during motor rehabilitation.

For the classifier to distinguish between movements, it was necessary to separate periods of rest and periods of movement in the signal. A Matlab code was written to detect time stamps for the beginning of each movement segment and each rest segment. Only the periods of movement were used in the

Fig. 1 Electrode Placement and Sample Signals. Illustrated are the positions of wireless Ag/AgCl electrodes on the subjects from the NINAPro Database. Each oval represents an electrode. The sample signals shown are a representation of the raw sEMG signal from each electrode during one movement. Each signal is on a y-axis of 0.001 mV and an x-xis of 6 seconds
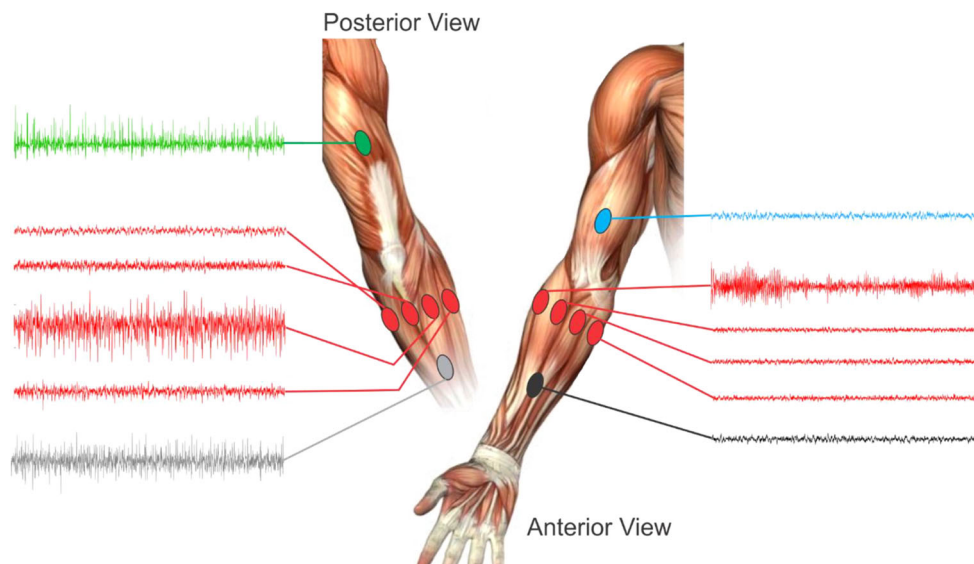
	Channel	Muscle
🟥	1-8	Equidistant electrodes around radio-humeral joint
⬛	9	Flexor Digitorum Superficialis
⬜	10	Extensor Digitorum Superficialis
🟦	11	Biceps Brachii
🟩	12	Triceps Brachii

remainder of this study. It is important to characterize how the muscle activity changes throughout dynamic movement. The amplitude and frequency of the signals change at different times for different muscles to complete a functional movement. With this in mind, each movement segment was divided to consider the non-stationarity of the signal frequency and amplitude. Multiple sets of time divisions were tested to identify the best total number to represent signal information. Dividing the signal into 3, 5, 10, and 20 segments separately, the statistical features were calculated and input into the classifiers. The classification accuracies were highest with the 3-segment divisions, and therefore, the signal was divided into thirds to signify the beginning, middle, and end of a movement. For each of these sub-segments, the mean amplitude and frequency of the signal was calculated. These time-domain parameters are the input data for the EPNN classifier to determine the type of movement.
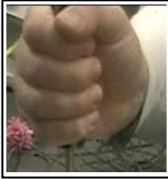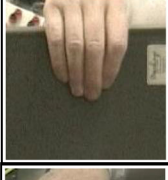
Feature Extraction

Time-frequency features were extracted from decomposed signals of each of the 12 channels used for each subject. Each signal was between 4 and 6 s long. The db4 wavelet from the Daubechies wavelet family was applied to conduct the discrete wavelet transform for signal decomposition into 5 levels. Both 5-level and 3-level DWT were applied for feature extraction. The use of 5 levels was determined based on the work of Subasi [45]. A similar study by Atzori et al. [5] used a 3 level DWT. In this study, the 5-level DWT

features provided the most accurate classification. While these feature bands are not directly physiologically correlated with motor unit frequencies in the arm, they can be used as a pseudospectrum of similar firing rates belonging to the motor units active during specific movements. Statistical parameters were calculated from each of these decomposed signals in an approach similar to that described in a recent study [45]: mean of the absolute value of wavelet coefficients, standard deviation of wavelet coefficients, the average power of the wavelet coefficients, and the ratios of the absolute mean value of adjacent sub bands. For each one of the five movements listed in Table 1, twelve channels of data were collected from the upper limb as depicted in Fig. 1. The breakdown of feature extraction from each channel of data is shown Fig. 2. Each channel is broken down into five levels using the DWT. Each level was broken down into 3 time segments. The mean, standard deviation, and power of the wavelet coefficients are calculated for each of the three time segments for all levels. This yielded a subtotal of 45 features for that channel. There were 8 ratios between the adjacent levels. In total, there were 53 features for each channel. The features for all 12 channels were included in a one distinguishing feature vector for one movement trial, yielding $53 \times 12 = 636$ unique features per movement.

The raw sEMG signal is decomposed into 5 levels using the discrete wavelet transform. The signal coefficients for each are plotted for d1 to d5, where d stands for details, which are the detailed levels provided by the wavelet transform. Statistical calculations for each level are calculated. The mean

Table 1 Association of the AMAT movements to movements available through the NINAPro Database. Dynamic movements available through the NINAPro Database and used in this study because they mimic the movements used in the AMAT for assessment of motor ability. Full AMAT list of movements available in Appendix Table 4

	AMAT Movement		Associated NINAPro Database Movement
1	**Telephone Grasp**		Small Diameter Grasp
2	**Doorknob grasp**		3-Finger Sphere Grasp
3	**Light switch (pincer) grasp**		Prismatic Pinch Grasp
4	**Foam Sandwich grasp**		Parallel Extension Grasp
5	**Cut Meat**		Cut Something

absolute value (MAV) of the amplitude for each level is calculated and compared to the adjacent levels using a ratio. The time scale is then broken into thirds for the mean, standard deviation, and power to be calculated. For each electrode channel, the mean, standard deviation, and power are calculated for each decomposition level and each time segment, accompanied by the ratios to complete the feature set for that channel during one movement.

Feature Analysis

A sensitivity analysis was conducted to determine the effect of feature subsets on each classifier. Feature subsets were divided based either on signal decomposition level or statistical calculations. The decomposed signal levels served as a pseudo-representation of the sub-signals that make up the sEMG signals collected. Time windows represent the beginning, middle, and end of a movement and were chosen to analyze different signal contributions at different time points during the movement. Statistical features were excluded one by one to analyze their relevance to movement identification. First the features were removed from the feature set based on decomposition level, time window, type of statistical measurement, and channel. For example, the features calculated for decomposition level 1 were removed from the feature set, leaving a subset of features containing all of the features from decomposition levels 2 through 5. This was done for all decomposition levels. To understand the contribution of the time segments, the first time segment was removed and the remaining feature subset consisted of all the features for the remaining time segments for all decomposition levels. This was done for all three time segments. Lastly, the statistical parameters were excluded. The mean calculations for all of the decomposition levels were excluded, leaving the feature subset to consist of the ratios, standard deviations, and power calculations. This was also done for power, standard deviations, and ratios separately. The new feature set, excluding a subset of features, were then input into the classifiers.

A second feature analysis was conducted to determine individual feature's contribution to classification accuracy. All
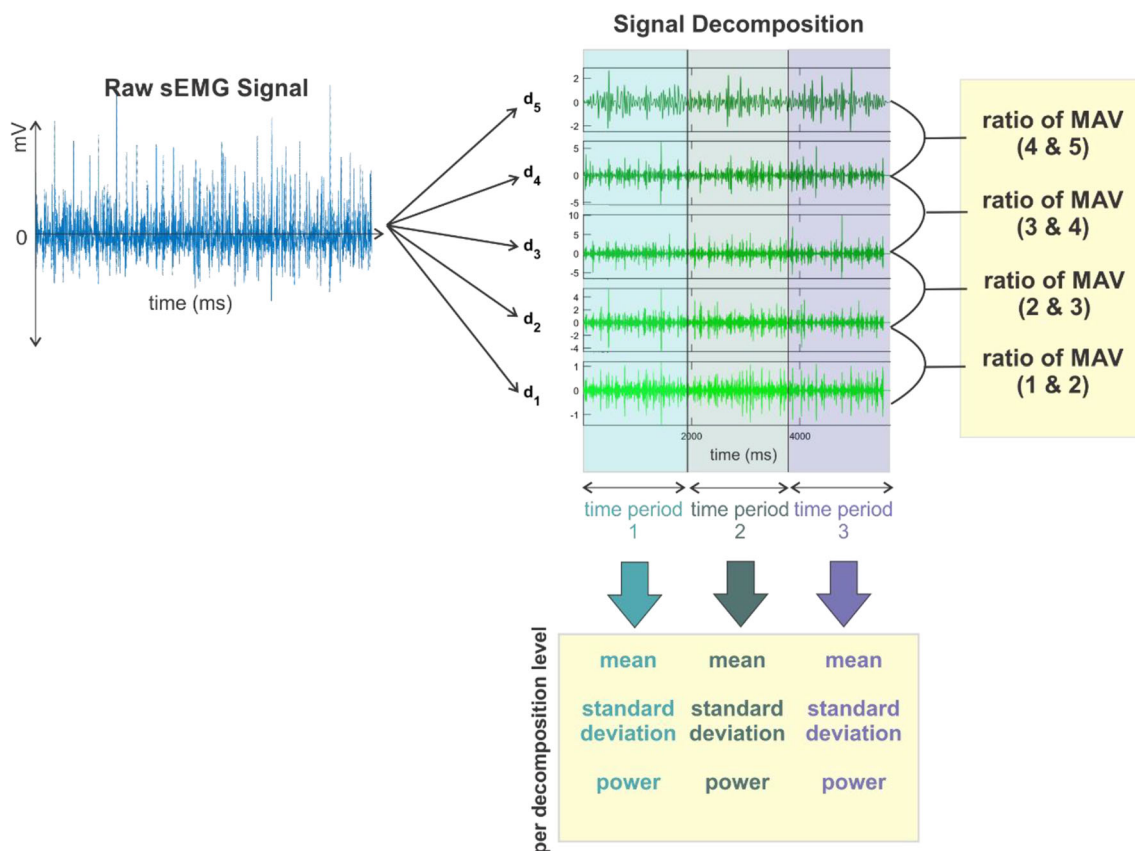
Fig. 2 Feature extraction breakdown. The raw sEMG signal is decomposed into 5 levels using the discrete wavelet transform. The signal coefficients for each are plotted for d1 to d5, where d stands for details, which are the detailed levels provided by the wavelet transform. Statistical calculations for each level are calculated. The mean absolute value (MAV) of the amplitude for each level is calculated and compared to the adjacent levels using a ratio. The time scale is then broken into thirds for the mean, standard deviation, and power to be calculated. For each electrode channel, the mean, standard deviation, and power are calculated for each decomposition level and each time segment, accompanied by the ratios to complete the feature set for that channel during one movement

combinations of features were tested to determine the optimal feature set. This totaled up to 1430 combinations. For 53 features from each channel, all amounts lower than 53 were input into the mathematical combination formula, n-choose-r. For example, all combinations for 52 features from the original feature set of 53 features were tested. The same was done for 50 features, 49 features, 48 features, and so on. The subset of features was input into EPNN to identify which feature set produced the highest accuracy.

Classification

Four machine learning techniques were employed for classification evaluation: SVM, k-NN, PNN, and EPNN. The original feature set consisted of 636 features for every movement trial. This included statistics for all DWT decomposition levels for each channel, with the overall time to complete the movement equally divided into three sections. Extracted features were fed into each classifier using a leave-one-out methodology, where the classifier was trained using all trials except

one for each movement on a subject-by-subject basis. Each classifier is described briefly in the following paragraphs.

PNN is a supervised, feed-forward neural network consisting of four layers: an input layer, a pattern layer, a summation layer, and an output layer. The input layer of PNN consisted of 636 neurons. The pattern layer uses a global Bayesian rule [24, 63] to determine the distance of testing data relative to the training data. The summation layer calculates the probability that testing data belongs to one of the indexed movement classes, which is then fed into a maximum likelihood function in the output layer to produce a class prediction. EPNN is an enhanced version of PNN which takes local information into consideration as well as global information in the pattern layer. Using local hyperspheres with a user-defined radius, the spread parameter is weighted by data points within this hypersphere in relation to the data point being assessed [1]. EPNN has proven to provide higher accuracies than PNN in the literature [3, 14, 22].

SVM is a supervised-learning technique that iteratively computes a vector that distinguishes features between classes [10]. It does this by calculating a non-linear vector, choosing

the largest distance between features of each class. It was applied here using a non-standardized feature set and trained on 5 out of the 6 trials for each movement. k-NN is another supervised-learning technique that can be used for classification. The "k" in k-NN represents the user-defined number of neighbors, or closest data to the unknown data point to be classified, and is chosen based on the nature of the data being classified. It relies on a majority voting system to determine to which class a test input belongs.

Results

Classification

Error bars represent the 95% confidence interval.

Each box contains a percentage of occurrences where one class was predicted for another class. This is done for each movement. The diagonal line represents the classification accuracies for each movement, i.e. when the predicted class matches the true class.

When classifying the five movements associated with the AMAT using all of the features described above, average within-subject accuracy was 73.8% for EPNN, 73% for PNN, 63% for SVM, and 61% for k-NN (Fig. 3). The highest accuracy was achieved using EPNN by setting the spread parameter to 0.01 and the local hypersphere radius to 0.001. The highest accuracy for k-NN was achieved using k = 3 and without feature standardization. The highest accuracy for SVM was achieved without standardization as well.

The EPNN classifier predicted movement #5 (cut something) for movement #1 (telephone grasp) 32% of the time, providing an accuracy of only 57% for movement #1 (Fig. 4). The remaining four movements were classified within an accuracy range of 77% - 85%. The large misclassification of
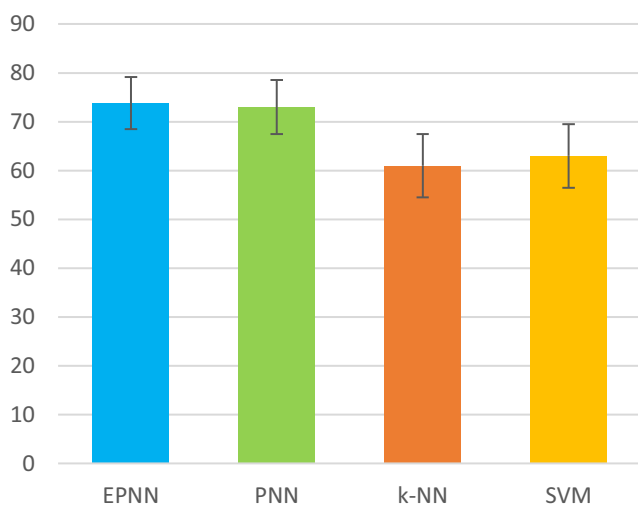

Fig. 4 EPNN Confusion Matrix. Each box contains a percentage of occurrences where one class was predicted for another class. This is done for each movement. The diagonal line represents the classification accuracies for each movement, i.e. when the predicted class matches the true class.

movement #1 brought down the overall accuracy of the EPNN classifier. This is likely due to the similarity in grip type to complete each task. The only difference between the telephone grasp and the cut something grasp is the extension of the pointer finger, which is better detected with muscles in the hand. While the misclassification of movement #1 as movement #5 occurs at a similar rate in both the SVM and k-NN classifiers, the overall accuracy is not heavily affected, as the accuracies for all five movements remain within 59% - 66% for SVM and 58% - 68% for k-NN.

Feature Analysis

Table 2 reports the effects on each classifier of excluding features from the feature set. Of the classifiers used in this study, EPNN is the best suited for determining a feature's weight on the model because it makes its decisions based on the distribution of features and the distance between them, whereas SVM and k-NN do not take both global and local information into account simultaneously. Removal of statistical features from 4 of the 5 decomposition levels caused a decrease in accuracy, indicating their importance to the classification decision. Removal of statistical features from any of the time divisions did not affect the accuracy at all, indicating they may not contain information pertinent to classification accuracy separate from each other. The most interesting finding is the effect of removing the types of statistical features regardless of decomposition level or time division. When removing the mean, standard deviation, or power calculations, the accuracy of classification showed no difference. However, when removing the ratio of adjacent decomposition level means, the accuracy of the classifier dropped significantly

Fig. 3 Within-Subject Classification Accuracy

Table 2 Feature Sensitivity Analysis Results The change in accuracy due to feature exclusion is reported here. The left column identifies the subset of features that were excluded from the overall feature set. All features related to the level, time division, or statistical calculation indicated in the leftmost column have been excluded and input into the three classification algorithms, EPNN, SVM, and k-NN

Change in Accuracy (%)

Excluded Features	EPNN	SVM	k-NN
Level 1	−4	0	−27
Level 2	−4	−3	−25.5
Level 3	−5	−3	−30.5
Level 4	−6	−3	−27
Level 5	0	−3	−27.5
Time Division 1	0	0	−32.5
Time Division 2	0	1	−27.5
Time Division 3	0	−1.5	−19
Mean	0	0.5	−24
Standard Deviation	0	0.5	−23.5
Power	0	−0.5	−28
Ratios	−54	−27	−27

by 54%. Because of the large effect the ratio features had, the classifiers were run using these features only.

The change in accuracy due to feature exclusion is reported here. The left column identifies the subset of features that were excluded from the overall feature set. All features related to the level, time division, or statistical calculation indicated in the leftmost column have been excluded and input into the three classification algorithms, EPNN, SVM, and k-NN.

Table 3 indicates the effect each channel has on the classification accuracy of each classifier. EPNN and k-NN showed decreases in accuracy consistently by removing a channel's worth of information, which indicates that information from

Table 3 Changes in accuracy determined by excluding subsets of signal features

Change in Accuracy (%)

Channel	EPNN	SVM	KNN
1	−1	−2.5	−28
2	−2	−2	−27.5
3	1	1.5	−27
4	−1	0.5	−25.5
5	−1	−1.5	−27
6	−1	1	−24
7	−3	−1	−26
8	−2	−3.5	−28.5
9	−1	−1 5	−27.5
10	−1	3	−26
11	−2	2	−27
12	−7	−1.5	−28

all channels are necessary for these two classifiers to make their most accurate predictions. SVM, however, showed increases in accuracy when removing 3 of the 8 forearm channels, biceps brachii channel, and extensor digitorum superficialis channels, which demonstrates these channels were not used to create the largest distinction among classes. A removal of any channel with k-NN created a decrease in accuracy between 24% - 28.5%, indicating the necessity of all channel information for this algorithm. Except for channel 3, one of the eight radio-humeral level forearm electrodes, removal of any channel in the EPNN classifier resulted in a decrease in accuracy as well, but not to the magnitude of k-NN. Removal of channel 12, the triceps brachii, caused the largest decrease in EPNN accuracy for classification. The best combination of features excluded one of the eight ratios of mean absolute values between decomposition levels. The ratio was that of decomposition levels 3 and 2. This yielded an average classification accuracy of 75.5%.

Discussion

EPNN outperformed other widely-used classification techniques with the sEMG feature set presented in the current study. Based on the classification accuracies, EPNN is a robust classifier for personalized movement classification. This has been shown previously with other biosignals in the literature, which further validates the robustness of EPNN. Identifying the ratios of adjacent decomposition levels as the most important feature in the presented feature set, all of the classifiers were re-run using only these features. This increased EPNN's accuracy to 74.4%. It is possible that increased accuracies could be achieved by identifying other features not used in the current study to be combined with these ratios. These ratio features being responsible for the majority of class differentiation could be explained by the nature of DWT decomposition, sEMG, and the frequency with which the brain activates the muscles for different movements, known as motor unit recruitment. Because sEMG is being recorded from the surface of the skin, the resolution of muscle signal measurement is low compared to EMG gathered using needle electrodes that interface directly with the muscles. sEMG gathers a summation of muscular activity produced by the multiple motor units within each muscle. By decomposing the sEMG signal into multiple frequency bands, this summation signal is broken down into banks that potentially represent motor units firing at similar frequencies. As the type of movement changes, the frequency and amplitude of muscle activation change, which provides potentially distinguishing features among movements.

The complexity of sEMG signals stem from the fluctuating frequencies and amplitudes from various motor units over time. This is the root cause of its non-stationary nature and

the reason advanced signal processing techniques are necessary for analyzing the true nature of these signals. The wavelet transform uses a pre-described wavelet with a varying frequency and amplitude to scale and stretch over the original signal. The output coefficients of the wavelet transform identify the signal's relationship to this wavelet to characterize the signal in the time and frequency domain simultaneously. In doing so, the non-stationary nature of the sEMG signal is addressed. Simply inputting all of the coefficients into a classifier as a feature set can be done, however, this is computationally expensive. By dividing the sEMG signal into three time divisions per movement, changes in the signal throughout the movements could be identified by features extracted from each of these segments. Statistical calculations of these time segments, ratios between decomposition levels, mean absolute value, standard deviation, and signal power, represent the signal changes over time and reduce the computational time from using all coefficients as inputs. The result of a zero change in accuracy when removing any features related to any of the three time divisions indicates the signal information for these movements does not drastically change over time such that the features derived from that information are distinguishable among movement classes.

Within the literature numerous studies use sEMG signals to classify upper limb movement for spinal cord injury patients and amputee patients. Most of these studies aim to increase the accuracy of myoelectric prosthetics for use of patients suffering from some level of motor dysfunction. For myoelectric prosthetics, distinguishing between fine motor movements are of utmost importance, for the target population are amputees who still have control over gross motor function and use myoelectric prosthetics for hand grasping motions. Multiple studies have reported the ability to distinguish between grasps solely using sEMG and machine learning classification techniques. For hand grasping movements in healthy subjects, accuracies reported range from 50 to 60% for k-Nearest Neighbors, 60–70% for support vector machines, and 70–75% for random forest classifiers [5, 6].

When comparing the present study to Liu et al. [30] it is important to note an exoskeleton can increase the precision of movements within and between subjects, allowing the training and testing samples to be more similar than that of upper limb movement without an exoskeleton. For both stroke and healthy subjects 98% of the variance between actual and predicted movement trajectories with the assistance of an exoskeleton robot to control the movements was accounted for [30]. Because the present study uses free, unsupported movement of the upper limb, the movement trajectories cannot be controlled, and therefore there is a larger variance within the data set. Another fact to consider is the difference in outputs for the neural networks between the two studies. Liu et al. [30] provide a continuous output of predicted numbers versus the classification of full functional movements in the present

study. The present study is the first to evaluate the capability of neural networks and other machine learning techniques to distinguish between sEMG signals of dynamic functional movements used for upper limb motor rehabilitation.

Differences in accuracy between studies depend heavily on the differences in input features chosen for each classification problem. Common features in the literature include root mean square, thresholded histograms, zero-crossings, mean average slopes, standard deviation, mean, and wavelet coefficients. The highest accuracies were achieved using root mean squares of sEMG signals and the ratios of interactions between co-contracting muscles for hand grasping movements [53]. Another difference between the two studies that should be noted, is the subject pool used. While both studies used NINAPro Database 2, Wei et al. [53] reduced their dataset to a subset of eight out of the forty subjects available, and the current study used all forty to calculate the average classification accuracy. This difference makes comparison between the two studies more complex. Nevertheless, it is possible that higher accuracies can be achieved using EPNN if coactivation ratios were included in a feature set with the decomposition ratios presented in this study using healthy subjects. Stroke patients suffering from motor dysfunction often also struggle with spasticity, an abnormal pattern of muscle recruitment associated with hyperactive stretch reflexes [49]. Spasticity causes abnormal coactivation patterns that are not observed in healthy movements [12]; therefore, using coactivation patterns as features might not perform well for sEMG movement classification in stroke patients. Classification approaches would need to be tested in stroke patients to determine which approaches perform best.

The main question for this study was, "Can movements used in stroke motor ability assessments be distinguished using EPNN?" After attempting multiple feature sets including the features listed earlier in this paragraph, the features reported in the results section produced the highest classification accuracy. While more advanced feature extraction techniques could potentially increase the classification accuracy further, an in depth analysis and comparison of feature extraction techniques is beyond the scope of this study.

Most studies classify gross motor function using isometric exercises, which consists of muscle contraction without joint movement [45]. Movement in daily life is dynamic. Dynamic movement involves muscle co-contraction and synergy as well as joint movement to complete functional tasks. Early studies in the literature that reported high accuracies of sEMG classification utilized isometric contraction of muscles [9]. The current study attempts to classify dynamic movement, which might be the reason for lower accuracy scores, but is one step closer to full understanding and utilization of dynamic movement measurement.

Further optimization of these approaches for application in motor rehabilitation after stoke could involve several

approaches. Adding more sEMG electrodes or altering their positions on the forearm compared to what was used in the NINAPro data would be a first step. In addition to recording from the forearm, adding electrodes that could measure at least some intrinsic muscles in the hand could prove particularly valuable. A combinatorial approach using sEMG along with motion sensors to detect aspects of forearm and hand movement could also be helpful. Moving beyond hand movements and forms of fine motor skill into broader distinctions of movements, such as reaching for and drinking a cup of water, operating a light switch, turning a doorknob, and sampling from a variety of more proximal muscles might provide a different challenge and would require a broader set of muscles. The scenario tested in the present study, a variety of manipulation tasks with a relatively small number of closely spaced electrodes only in the forearm, represents a relatively difficult problem with which to test the performance of the classification approaches. Given that the EPNN performs best in this challenging scenario, it would be interesting to determine if it also performs best for classifying a wider variety of movements. The research presented in this paper is a step in that direction.

Conclusion

The present study has demonstrated the capability of using upper limb sEMG signals to identify and distinguish between functional movements used in standard upper limb motor assessments for stroke patients. This was accomplished through adroit integration of signal processing, feature extraction, and machine learning classification. Many studies in the literature utilize wavelet decomposition to enhance feature extraction for class identification. However, the importance of the amplitude relationship between wavelet decomposition levels, referred to as the ratio features in the methods section, was demonstrated in the current work. Having outperformed SVM, k-NN, and PNN, EPNN is shown as a strong contender for current popular techniques used for machine learning classification in the literature.

Using sEMG signals to classify movement has many applications within the field of motor rehabilitation for stroke patients. The ability to classify movements used within the AMAT can provide clinicians with quantitative information to support diagnosis and progression monitoring of stroke patients throughout rehabilitation techniques. Separately, with the proper wireless sEMG setup, daily monitoring of movement can provide a quantitative method for analyzing functional movements of stroke patients at home, a practice known to enhance motor rehabilitation outcomes. By classifying movements via sEMG, information can be relayed to clinicians and researchers for better understanding of how daily movement outside of the clinic contributes to motor recovery.

Compliance with Ethical Standards

Authors declare that they have no conflict of interest. Authors did not collect data from humans or animals. Data used in this research are from publicly-available sources.

Appendix 1

Table 4   The table below lists the 10 movements used for the AMAT as adapted by O'Dell et al. [38]. This adaptation reduced the number of movements to be performed from 13 to 10 to increase the clinical viability of the test for stroke patient movement completion. The 5 movements used in the present study are highlighted in bold font

Arm Motor Ability Test (AMAT)

Task	Description
Cut Meat	**A. Pick up knife and fork** **B. Cut Meat** C. Fork to mouth
Foam Sandwich	**A. Pick up Foam Sandwich** B. Sandwich to mouth
Eat with Spoon	A. Pick up spoon B. Pick up bean with spoon C. Spoon to mouth
Comb Hair	A. Pick up comb B. Comb hair
Open Jar	A. Grasp jar top B. Screw jar top open
Tie Shoelace	A. Tie Shoelace
Use Telephone	A. Phone receiver to ear B. Press phone number
Put on T-shirt	A. Arms in T-shirt sleeve B. Head through hole C. Pull down and straighten shirt
Light Switch/Door	A. **Pincer grasp of light switch** and flip down B.**Grasp door handle,** rotate handle, open door C. Close door

References

1. Ahmadlou, M., and Adeli, H., Enhanced probabilistic neural network with local decision circles: A robust classifier. *Integr Comput-Aided Eng*. 17(3): 197–210, 2010. https://doi.org/10.3233/ICA-2010-0345.
2. Alexandridis, A., Paizis, E., Chondrodima, E., and Aliaj, E., A particle swarm optimization approach in printed circuit board thermal design. *Integr. Comput-Aided Eng*. 24(2):143–155, 2017.
3. Amezquita-Sanchez, J. P., Adeli, A., and Adeli, H., A new methodology for automated diagnosis ofmild cognitive impairment (MCI) using magnetoencephalography (MEG). *Behav. Brain Res*. 305:174–180, 2016. https://doi.org/10.1016/j.bbr.2016.02.035.
4. Ansari, A. H., Cherian, P. J., Caicedo, A., Naulaers, G., De Vos, M., and Van Huffel, S., Neonatal seizure detection using deep convolutional neural networks, *Int. J. Neural Syst*. 29(4):1850011, 2019.
5. Atzori, M., Gijsberts, A., Castellini, C., Caputo, B., Hager, A.-G. M., Elsig, S., and Müller, H., Electromyography data for non-

invasive naturally-controlled robotic hand prostheses. *Sci Data*. 1: 140053, 2014. https://doi.org/10.1038/sdata.2014.53.

6. Atzori, M., Cognolato, M., and Müller, H., Deep learning with convolutional neural networks applied to electromyography data: A resource for the classification of movements for prosthetic hands. *Front. Neurorobot.* 10(SEP), 1–10, 2016. https://doi.org/10.3389/fnbot.2016.00009.

7. Cesqui, B., Tropea, P., Micera, S., and Krebs, H. I., EMGbased pattern recognition approach in post stroke robot-aided rehabilitation:a feasibility study. J. Neuroeng. Rehabil, 10(1):75, 2013. https://doi.org/10.1186/1743-0003-10-75.

8. Chen, M., Zhang, X., Lu, Z., Li, X., and Zhou, P., Two-source validation of progressive fastica peel-off for automatic decomposition of high density surface EMG. *Int. J. Neural Syst.* 28:9 (14 pages), 2018.

9. Chu, J. U., Moon, I., and Mun, M. S., A real-time EMG pattern recognition system based on linear-nonlinear feature projection for a multifunction myoelectric hand. *IEEE Trans. Biomed. Eng.* 53(11):2232–2239, 2006 https://doi.org/10.1109/TBME.2006.883695.

10. Dai, H. and Cao, Z., A wavelet support vector machine based neural network meta model for structural reliability assessment. *Comput-Aided Civ. Infrastruct. Eng.* 32(4):344–357, 2017.

11. Dai C., and Hu, X., Extracting and classifying spatial muscle activation patterns in flexor digitorum superficialis using high-density electromyogram recordings. *Int. J. Neural Syst.* 29(1): 1850025 (15 pages), 2019.

12. Dewald, J. P., Pope, P. S., Given, J. D., Buchanan, T. S., and Rymer, W. Z., Abnormal muscle coactivation patterns during isometric torque generation at the elbow and shoulder in hemiparetic subjects. *Brain*. 118(Pt 2):495–510, 1995. https://doi.org/10.1093/brain/118.2.495.

13. Gaur, P., McCreadie, K., Pachori, R. B., Wang, H., and Prasad, G., Tangent space feature-based transfer learning classification model for two-class motor imagery brain-computer interface. *Int. J. Neural Syst.* 29(10):19500215 (17 pages), 2019.

14. George, S. H., Rafiei, M. H., Borstad, A., Gauthier, L., Buford, J. A., and Adeli, H., Computer-aided prediction of extent of motor recovery following constraint-induced movement therapy in chronic stroke. *Behav. Brain Res.* 327:191–199, 2017.

15. Ghosh-Dastidar, S., Adeli, H., and Dadmehr, N., Principal component analysis-enhanced cosine radial basis function neural network for robust epilepsy and seizure detection. *IEEE Trans. Biomed. Eng.* 55(2):512–518, 2008.

16. Gok, S. and Sahin, M., Prediction of forelimb EMGs and movement phases from corticospinal signals in the rat during the reach-to-pull task. *Int. J. Neural Syst.* 29(7):1950009 (20 pages), 2019.

17. Gómez-Vilda, P., Gómez-Rodellar, A., Ferrández Vicente, J. M., Mekyska, J., Palacios-Alonso, D., Rodellar-Biarge, V., Álvarez-Marquina, A., Eliasova, I., Kostalova, M., and Rektorova, I., Neuromechanical modelling of articulatory movements from surface electromyography and speech formants. *Int. J. Neural Syst.* 29(2):1850039 (17 pages), 2019.

18. Gorriz, J. M., Ramirez, J., Segovia, F., Martinez, F. J., Lai, M. C., Lombardo, M. V., Baron-Cohen, S., and Suckling, J., A machine learning approach to reveal the neuro-phenotypes of autisms. *Int. J. Neural Syst.*. 1850058:(22 pages), 2019.

19. Gray, V. L., Ivanova, T. D., and Garland, S. J., A single session of open kinetic chain movements emphasizing speed improves speed of movement and modifies postural control in stroke. *Physiother. Theory Pract.*. 614: 1–11, 2016. https://doi.org/10.3109/09593985.2015.1110848.

20. Gresham, G., Duncan, P., and Stason, W., *Post-stroke rehabilitation*. Darby, PA: Diane Publishing, 2004.

21. Hayward, K. S., Eng, J. J., Boyd, L. A., Lakhani, B., Bernhardt, J., and Lang, C. E., Exploring the role of accelerometers in the measurement of real world upper-limb use after stroke. *Brain Impair*. 1(314):1–18, 2015. https://doi.org/10.1017/BrImp.2015.21.

22. Hirschauer, T. J., Adeli, H., and Buford, J. A., Computer-aided diagnosis of parkinson's disease using enhanced probabilistic neural network. *J. Med. Syst.* 39(11), 2015. https://doi.org/10.1007/s10916-015-0353-9.

23. Hua, C., Wang, H., Wang, H., Lu, S., Liu, C., and Khalid, S. M., A Novel method of building functional brain network using deep learning algorithm with application in proficiency detection. *Int. J. Neural Syst.*. 29(1):1850015 (17 pages), 2019.

24. Huang, Y., and Beck, J. L., Full Gibbs sampling procedure for Bayesian system identification incorporating sparse Bayesian learning with automatic relevance determination. *Comput-Aided Civ. Infrastruct. Eng.* 33(9):712–730, 2018.

25. Khedher, L., Illan, I. A., Gorriz, J. M., Ramirez, J., Brahim, A., and Meyer-Baese, A., Independent component analysis-support vector machine-based computer-aided diagnosis system for alzheimer's with visual support. *Int. J. Neural Syst.* 27:3, 1650050 (18 pages), 2017.

26. Klomp, A., and Van der Krogt, J., Design of a concise and comprehensive protocol for post stroke neuromechanical assessment. *J. Bioeng. Biomed. Sci.* (January 2011), 1–8, 2012. https://doi.org/10.4172/2155-9538.S1-008.

27. Lambach, R. L., Young, J. W., Flanigan, D. C., Siston, R. A., and Chaudhari, A. M. W., Knee joint loading during lineman-specific movements in american football players. 142–148, 2015.

28. Leuenberger, K., Gonzenbach, R.,Wachter, S., Luft, A., and Gassert, R., A method to qualitatively assess arm use in stroke survivors in the home environment. *Med. Biol. Eng. Comput.* 55(1), 1–10, 2016. https://doi.org/10.1007/s11517-016-1496-7.

29. Li, Z., Guiraud, D., Andreu, D., Gelis, A., Fattal, C., and Hayashibe, M., Real-time closed-loop functional electrical stimulation control of muscle activation with evoked electromyography feedback for spinal cord injured patients. *Int. J. Neural Syst.* 28(6): 1750063 (14 pages), 2018.

30. Liu, J., Kang, S. H., Xu, D., Ren, Y., Lee, S. J., and Zhang, L. Q., EMG-Based continuous and simultaneous estimation of arm kinematics in able-bodied individuals and stroke survivors. *Front. Neurosci.* 11(August):1–11, 2017. https://doi.org/10.3389/fnins.2017.00480.

31. Lorussi, F., Nicola, C., De Rossi D., Paradiso, R., Veltink, P., and Tognetti, A., Wearable textile platform for assessing stroke patient treatment in daily life conditions. *Front. Bioeng. Biotechnol.* 4:28, 2016.

32. Ma, X., Yu, N., and Zhou, W., Using dictionary pair learning for seizure detection, *Int. J. Neural Syst.* 29(4)1850005 (14 pages), 2019.

33. Manzanera, M. O., Meles, S. K., Leenders, K. L., Renken, R. J., Pagani, M., Arnaldi, D., Nobili, F., Obeso, I., Oroz, M. R., Morbelli, S., and Maurits, N. M., Scaled subprofile modeling and convolutional neural networks for the identification of Parkinson's disease in 3D nuclear imaging data. *Int. J. Neural Syst.* 29(9): 1950010 (15 pages), 2019.

34. Martinez-Mozos, O., Sandulescu, V., Andrews, S., Bellotto, N., Dobrescu, R., and Ellis, D., Stress detection using wearable physiological and sociometric sensors. *Int. J. Neural Syst.* 27:2, 1650041 (16 pages), 2017.

35. Martinez-Murcia, F.J., Gorriz, J.M., Ramirez, J., and Ortiz, A., Convolutional neural networks for neuroimaging in parkinson's disease: is preprocessing needed?. *Int. J. Neural Syst.* 28(10): 1850035 (18 pages), 2018.

36. Masse, F., Gonzenbach, R., Paraschiv-Ionescu, A., Luft, A., and Aminian, K., Wearable barometric pressure sensor to improve postural transition recognition of mobility – impaired stroke patients.

IEEE Trans. Neural Syst. Rehabil. Eng. 24(11): 1210–1217, 2016. https://doi.org/10.1109/TNSRE.2016.2532844.

37. Molina-Cabello, M. A., Luque-Baena, R. M., López-Rubio, E., and Thurnhofer-Hemsi, K., Vehicle type detection by ensembles of convolutional neural networks operating on super-resolved images. *Integr. Comput-Aided Eng.* 25(4:321–333, 2018.

38. O'Dell, M. W., Kim, G., Rivera, L., Fieo, R., Christos, P., Polistena, C., Fitzgerald, K., and Gorga, D., A psychometric evaluation of the arm motor ability test. *J Rehabil Med.* 45(6):519–527, 2013.

39. Patel, S., Hughes, R., and Hester, T., A novel approach to monitor rehabilitation outcomes in stroke survivors using wearable technology. *Proc. IEEE.* 98(3):450–461, 2010. https://doi.org/10.1109/JPROC.2009.2038727.

40. Phinyomark, A., Quaine, F., Charbonnier, S., Serviere, C., Tarpin-Bernard, F., and Laurillau, Y., EMG feature evaluation for improving myoelectric pattern recognition robustness. *Expert Syst. Appl.* 40(12):4832–4840, 2013. https://doi.org/10.1016/j.eswa.2013.02.023.

41. Ramos-Murguialday, A., Broetz, D., Rea, M., Läer, L., Yilmaz, O., Brasil, F. L., and Birbaumer, N., Brain–machine interface in chronic stroke rehabilitation: A controlled study. *Ann. Neurol.* 74(1), 100–108, 2013.

42. Rembado, I., Castagnola, E., Turella, L., Ius, T., Budai, R., Ansaldo, A., Angotzi, G.N., de Bertoldi, F., Ricci, D., Skrap, M., and Fadiga, L., Independent component decomposition of human somatosensory evoked potentials recorded by micro-electrocorticography. *Int. J. Neural Syst.* 27(4):1650052 (16 pages), 2017.

43. Sankari, Z. and Adeli, H., Probabilistic neural networks for EEG-based diagnosis of alzheimer's disease using conventional and wavelet coherence. *J. Neurosci. Methods.* 197(1):165–170, 2011.

44. Sengur, A., Akbulut, Y., Guo, Y., and Bajaj, V., Classification of amyotrophic lateral sclerosis disease based on convolutional neural network and reinforcement sample learning algorithm. *Health Inf. Sci. Syst.* 5(1): 9, 2017. https://doi.org/10.1007/s13755-017-0029-6.

45. Subasi, A. (2012). Classification of EMG signals using combined features and soft computing techniques. Appl Soft Comput J, 12(8), 2188–2198. https://doi.org/10.1016/j.asoc.2012.03.035.

46. Thielbar, K. O., Triandafilou, K. M., Fischer, H. C., O'Toole, J. M., Listenberger, M. L., Ochoa, J. M., Kamper, D. G. Benefits of using a voice and EMG-driven actuated glove to support occupational therapy for stroke survivors. *IEEE Trans. Neural Syst. Rehabil. Eng.* 4320(c):1–1, 2016. https://doi.org/10.1109/TNSRE.2016.2569070.

47. Torres, J. F., Galicia, A., Troncoso, A., and Martínez-Álvarez, F., Ascalable approach based on deep learning for big data time series forecasting. *Integr. Comput-Aided Eng.* 25(4):335–348, 2018.

48. Tosin, M. C., Majolo, M., Chedid, R., Cene, V. H., and Balbinot, A., SEMG feature selection and classification using SVMRFE. *Proceedings of the Annual International Conference of the IEEE Engineering in Medicine and Biology Society, EMBS.* 390–393, 2017. https://doi.org/10.1109/EMBC.2017.8036844.

49. Twitchell, T. E., The restoration of motor function following hemiplegia in man. *Brain.* 74(4): 443–480, 1951.

50. Vera-Olmos, F. J., Pardo, E., Melero, H., and Malpica, N. (2019), DeepEye: Deep convolutional network for pupil detection in real environments, *Integr. Comput-Aided Eng.* 26(1): 85–95.

51. Wang, P., and Bai, X. (2018). Regional parallel structure based CNN for thermal infrared face identification. *Integr. Comput-Aided Eng.* 25(3):247–260.

52. Wang, S., Hu, Y., Shen, Y., and Li, H., classification of diffusion tensor metrics for the diagnosis of a myelopathic cord using machine learning. *Int. J. Neural Syst.* 28(2), 2018.

53. Wei, J., Meng, Q., and Badii, A., Classification of human hand movements using surface EMG for myoelectric control. *Adv. Intell. Syst. Comput.* 513:331–339, 2017. https://doi.org/10.1007/978-3-319-46562-3_22.

54. Wolf, S., Winstein, C., Miller, J., Thompson, P., Taub, E., and Uswatte, G. (2008). The Excite trial: retention of improved upper extremity function among stroke survivors receiving CI Movement therapy. *Lancet Neurol.*, 7(1):33–40. https://doi.org/10.1016/S1474-4422(07)70294-6.

55. Wu, Q., Mao, J. F.,Wei, C. F., Fu, S., Law, R., Ding, L., … and Yang, C.H., Hybrid BF-PSO and fuzzy support vector machine for diagnosis of fatigue status using EMG signal features. *Neurocomputing.* 173:483–500, 2016. https://doi.org/10.1016/j.neucom.2015.06.002.

56. Wu, Q., Zhang, Y., Liu, J., Sun, J., and Cichocki, A., Regularized group sparse discriminant analysis for P300-based brain computer interface. *Int. J. Neural Syst.* 29(6):1950002 (15 pages), 2019.

57. Xia, P., Hu, J., and Peng, Y., EMG-based estimation of limb movement using deep learning with recurrent convolutional neural networks. *Artif. Organs.* 42(5):E67–E77, 2018. https://doi.org/10.1111/aor.13004.

58. Xue, Y. D. and Li, Y. C., A Fast detection method via region-based fully convolutional neural networks for shield tunnel lining defects. *Comput-Aided Civ. Infrastruct. Eng.* 33(8):638–654, 2018.

59. Yang, X., Li, H., Yu, Y., Luo, X., Huang, T., Yang, X., and Yang, X., Automatic pixel-level crack detection and measurement using fully convolutional network. *Comput-Aided Civ. Infrastruct. Eng.* 33:12, 2018.

60. Yang, T., Cappelle, C., Ruichek, Y., and El Bagdouri, M., Multi-object tracking with discriminant correlation filter based deep learning tracker. *Integr. Comput-Aided Eng.* 26(3):273–284, 2019.

61. Yu, B., Wang, H., Shan, W., and Yao, B. Prediction of bus travel time using random forests based on near neighbors. *Comput-Aided Civ. Infrastruct. Eng.* 33(4):333–350, 2018.

62. Zhang, Z., Fang, Q., and Gu, X., Objective assessment of upper limb mobility for post-stroke rehabilitation. *IEEE Trans. Biomed. Eng.* 63(4):859–868, 2016. https://doi.org/10.1109/TBME.2015.2477095.

63. Zhang, Y., Wang, Y., Jin, J., and Wang, X. Sparse Bayesian Learning for obtaining sparsity of EEG frequency bands based feature vectors in motor imagery classification. *Int. J. Neural Syst.* 27(2):1650032 (13 pages), 2017.

64. Zhang, X., Foderaro, G., Henriquez, C., and Ferrari, S., A scalable weight-free learning algorithm for regulatory control of cell activity in spiking neuronal networks. *Int. J. Neural Syst.* 28(2):1750015, 2018. https://doi.org/10.1142/S0129065717500150.

65. Zhang, J., Xiao, M., Gao, L., Chu, S., Probability and interval hybrid reliability analysis based on adaptive local approximation of projection outlines using support vector machine. *Comput-Aided Civ. Infrastruct. Eng.* 34(11):991–1009, 2019.